AD-A116 265 ARIZONA UNIV TUCSON ENGINEERING EXPERIMENT STATION F/G 20/4
AN EFFECTIVE ALGORITHM FOR SHOCK-FREE WING DESIGN.(U)
JUN 81 K FUNG, A R SEEBASS, L J DICKSON N00014-76-C-0182
UNCLASSIFIED TFD-81-06 NL

END
DATE
FILMED
8-82
DTIC

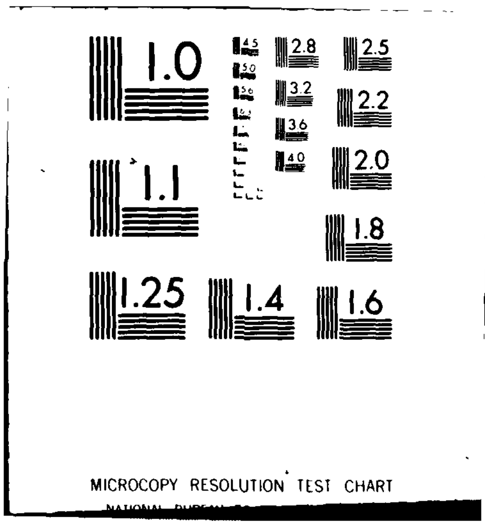
1.0
1.1
1.25
1.4
1.6
1.8
2.0
2.2
2.5
2.8
3.2
3.6
4.0
MICROCOPY RESOLUTION TEST CHART

AD A116265

TRANSONIC FLUID DYNAMICS

Report TFD 81-06

K. Y. Fung, A. R. Seebass,
L. J. Dickson, C. F. Pearson

AN EFFECTIVE ALGORITHM
FOR SHOCK-FREE WING DESIGN

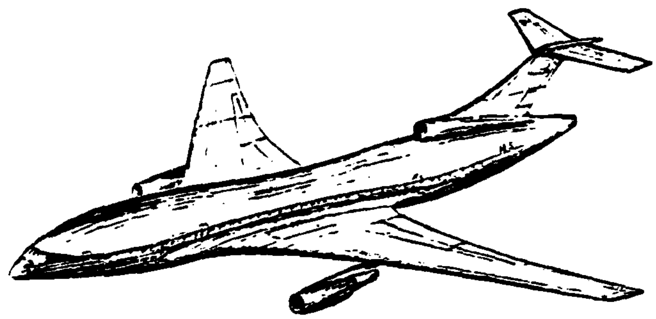

June 1981

ENGINEERING EXPERIMENT STATION
COLLEGE OF ENGINEERING
THE UNIVERSITY OF ARIZONA
TUCSON, ARIZONA 85721

SECURITY CLASSIFICATION OF THIS PAGE (When Data Entered)

REPORT DOCUMENTATION PAGE		READ INSTRUCTIONS BEFORE COMPLETING FORM
1. REPORT NUMBER	2. GOVT ACCESSION NO.	3. RECIPIENT'S CATALOG NUMBER
4. TITLE (and Subtitle) AN EFFECTIVE ALGORITHM FOR SHOCK-FREE WING DESIGN		5. TYPE OF REPORT & PERIOD COVERED
		6. PERFORMING ORG. REPORT NUMBER TFD 81-06
7. AUTHOR(s) K.-Y. Fung, A. R. Seebass, L. J. Dickson, and C. F. Pearson		8. CONTRACT OR GRANT NUMBER(s) N00014-76-C-0182
9. PERFORMING ORGANIZATION NAME AND ADDRESS University of Arizona Aerospace and Mechanical Engineering Tucson, Arizona 85720		10. PROGRAM ELEMENT, PROJECT, TASK AREA & WORK UNIT NUMBERS
11. CONTROLLING OFFICE NAME AND ADDRESS Office of Naval Research (code 438) Arlington, Virginia 22217		12. REPORT DATE June 1981
		13. NUMBER OF PAGES 28
14. MONITORING AGENCY NAME & ADDRESS(if different from Controlling Office) Office of Naval Research Resident Representative Room 223 Bandelier Hall West University of New Mexico Albuquerque, NM 87131		15. SECURITY CLASS. (of this report) Unclassified
		15a. DECLASSIFICATION/DOWNGRADING SCHEDULE

16. DISTRIBUTION STATEMENT (of this Report)

Approved for Public Release: distribution unlimited.

17. DISTRIBUTION STATEMENT (of the abstract entered in Block 20, if different from Report)

18. SUPPLEMENTARY NOTES

19. KEY WORDS (Continue on reverse side if necessary and identify by block number)

Wing Design
Airfoil Design

20. ABSTRACT (Continue on reverse side if necessary and identify by block number)

This paper reviews the fictitious gas procedure of Sobieczky for finding shock-free airfoils and wings. Results for inviscid and viscous flows for airfoils and wings are described. The method is applied to a business jet planform resulting in a wing that should have good low speed characteristics as well as an M_∞ L/D that is near the maximum achievable for the wing lift and thickness chosen for the study.

DD FORM 1 JAN 73 1473 EDITION OF 1 NOV 65 IS OBSOLETE
S/N 0102-014-6601

SECURITY CLASSIFICATION OF THIS PAGE (When Data Entered)

AIAA at 50

Anniversary Celebration

AIAA-81-1236
An Effective Algorithm for Shock-Free Wing Design

K. Y. Fung and A. R. Seebass, University of Arizona, Tucson, AZ; and L. J. Dickson, University of Washington, Seattle, WA; and C. F. Pearson, Harvard University, Cambridge, MA

AIAA 14th Fluid and Plasma Dynamics Conference

June 23-25, 1981/Palo Alto, California

AN EFFECTIVE METHOD FOR SHOCK-FREE WING DESIGN

K.-Y. Fung, A. R. Seebass, L. J. Dickson, and C. F. Pearson

Abstract

This paper reviews the fictitious gas procedure of Sobieczky for finding shock-free airfoils and wings. Results for inviscid and viscous flows for airfoils and wings are described. The method is applied to a business jet planform resulting in a wing that should have good low speed characteristics as well as an $M_\infty L/D$ that is near the maximum achievable for the wing lift and thickness chosen for the study.

INTODUCTION

There are a number of advancing technologies that should provide about a 40% improvement in transport aircraft fuel efficiency for the post 757/767 generation of aircraft. These include advances in the propulsion system, improved operations - including air traffic control-, composite materials for primary as well as secondary structures, active flight control, and supercritical aerodynamics. More than half of this improvement will come from the use of composite materials and active control, in conjuction with aeroelastic tailoring of the wing structure to suppress flutter. This paper addresses a more modest contributor to this expected gain, viz., supercritcal aerodynamics. Here we look for improvements in the "aerodynamic efficiency," $M_\infty L/D$, of about 5%. We must keep in mind that such small improvements are essential in obtaining the composite advance suggested above, and further, that each 1% increase in $M_\infty L/D$ of a single 300 passenger transport aircraft will save about $100,000 in fuel costs per year at present prices.

The goal of maximizing $M_\infty L/D$ requires aircraft wings that have shock-free flow over them for as large a Mach number as possible for fixed lift, thickness, etc. Such flows are mathematically isolated from one another and have, in the past, been difficult to find. In the late 1960s and early 1970s methods for generating airfoils that were shock free at supercritical Mach numbers were developed by Nieuwland (1), Bauer, Garabedian and Korn (2), and Sobieczky (3). These investigations used different techniques to the same end, and will not be reviewed here. But even in their most advanced state they did not provide a rich selection of airfoils and none could be generalized to three dimensions. The application of these airfoil designs to swept, three-dimensional wings, required cut and try modifications of the wing in order to even come close to achieving shock-free flow. But Sobieczky (4), in a brilliant generalization of his earlier approach, saw that finding such designs in two dimensions would be routine, and that it seemed this generalization would apply to three-dimensional flows as well (5). We now know that while this generalization leads to an ill-posed boundary-value problem in three dimensions, this causes no serious difficulty for wings of moderate to large aspect ratio (6).

This paper reviews the fictitious gas method of designing shock-free wings, illustrating the procedure with several codes now in common use in the aircraft industry. The authors know little of the overall design process and our focus is more properly on the minor modifications to a wing that is already optimized for low speed and subcritcal flight. The aerodynamic aspects of the design of commercial transports for aerodynamic efficiency have recently been reviewed by Lynch (7). We begin with the presumption that the designer has already chosen his basic airfoil section and wing planform and that he now wishes to maximize the $M_\infty L/D$ of the configuration using his existing computational tools, and that only a limited portion of the upper surface of the wing can be modified to achieve this goal without affecting the airfoil's low speed $(C_L)_{max}$. For our study we will use the GA(W)-2 airfoil and the Gates Learjet Century series planform.

AIRFOIL DESIGN

As noted above we begin by choosing a baseline airfoil. The GA(W)-2 has good low speed performance as well as some claim to being a relatively good supercritical airfoil (8). The numerical algorithm developed by Melnik (9) for computing the flow past airfoils in the presence of inviscid-viscous interactions, GRUMFOIL, has had early domestic dissemination. Nebeck (10) has modified this code for shock-free airfoil design in the presence of viscous interactions. N. Conley (private communication) reports that a modification of the Learjet wing section to obtain a shock-free flow at a freestream Mach number of 0.81 and a lift coefficient of $C_L = 0.50$ is desirable if this can be done with an airfoil such as the GA(W)-2 which has good low speed characteristics. Cosentino (private communication) has addressed the problem of design for an airfoil Mach number of 0.77 corresponding to a planform sweep of 15.7°. This process is not described here as the details may be found in Ref. 5, and our main concern is with wing design. With an appropriately chosen baseline airfoil based on the GA(W)-2, Cosentino was able to design an airfoil that was identical to the GA(W)-2 for the first 9% of its chord in order to retain the good low speed performance of the GA(W)-2, but had slight modifications to its upper surface in order to produce shock-free flow. Figure 1 compares the flow past the designed airfoil, GA(C)-250, as computed by GRUMFOIL, with that past a GA(W)-2 airfoil that has had its ordinates reduced to provide an 11.7% thick airfoil [GA(W)-2T]. The design point is $M_\infty = 0.7725$ and $C_L = 0.50$ with $Re = 6 \cdot 10^6$. Figure 2 compares the skin friction and boundary-layer displacement thickness on the two airfoils; note the small region of separation on the GA(W)-2T which has led to the lambda shock configuration responsible for the pressure distribution in Figure 1. We infer from these results that about a 100 count drag reduction has been achieved. The GA(W)-2, GA(C)-250, and the GA(W)-2T airfoils are compared in Figure 3. While there are only minor differences among the GA(W)-2T and GA(C)-250 airfoils, there are major differences in their supercritical performance indicating the great sensitivity of the flow to very minor changes in the upper surface. Since the GA(C)-250 is identical to the GA(W)-2 for the first 9% of the chord, we expect that it will also have a good low speed $(C_L)_{max}$.

WING DESIGN

Having selected our baseline airfoil, we now turn to wing design. We use this airfoil in the wing generator code of Sobieczky (11) to generate the wing input for a three - dimensional computation. We have chosen the FLO22 algorithm of Jameson and Caughey (12) for our wing studies. This code is well accepted by industry and is considerably faster than the conservative finite volume code used by Yu (13) to the same end. We note that while conservative differencing is important in the capture of shock waves, our design procedure computes the solution to an elliptic system and this can be done accurately with a nonconservative code. The basic tenets of the procedure have been descibed elsewhere (6,14). Because the changes we will make to our wing sections will be small, we must be careful to be sure they do not become obscured in the mapping from the physical plane to the computational plane. We have thus included a recomputation of the flow field after the design process in the computational variables in order to verify the results.

We remind the reader that in three-dimensions we solve an ill-posed boundary-value problem, and that any three-dimensional design must be confirmed by an analysis of the flow past this wing. The results of this computation are then compared with an analysis of the original wing shape, again using FLO22. Here, when there are shock waves present in the flow, this nonconservative calculation may overestimate their strength somewhat; however, the conservative potential approximation is even worse in this regard.

We begin our study with the candidate wing generated by the wing generator from the candidate baseline airfoil. Recall that this baseline airfoil was derived from the airfoil section of the wing we have designed to have optimum subcritical performance; it is not the airfoil we have designed to be shock free. We now repeat our fictitious gas study with a gas law that is close to that used in the airfoil design process. For conservative calculations we use a fictitious density, ρ_f, that depends on the flow speed q in a simple power law fashion, viz., $\rho_f / \rho_\infty = (q^*/q)^P$ for $q > q^*$, where $P < 1$, and is typically 0.9. In nonconservative calculations we prescribe a fictitious sound speed a, where $a = q(q/q^*)^L$ and $L > 0$. A value of $L = 5$ gives results similar to those of $P = 0.9$. Note that changing L (or P) results in a change in the size of the upper surface of the wing wetted by supersonic flow with the lower values of L (and higher values of P) reduce this area because they increase the mass flow through a unit area of the sonic surface.

Our goal, then, is to maximize $M_\infty L/D$ within the constraint that we maintain the features of the wing that optimized its subcritical performance. This we do by modifying the baseline airfoil and fictitious gas laws. We may even wish to employ an inverse design procedure like that of Henne (15) with the fictitious gas in order to help locate the fictitious supersonic domain where we wish it on the upper wing surface. Generally, the process of finding such a design requires several changes in the baseline section definition, additional changes in the twist variation to achieve an elliptic load distribution, and perhaps a half dozen Mach number and angle of attack changes to determine the maximun M_∞ for which shock-free flow can be found for a given lift. Figure 4 depicts the pressures and corresponding wing sections for a non-shock-free wing design based on the GA(W)-2T airfoil. The wing has a lift coefficient of 0.375 at M_∞ = 0.80 and a nominal thickness of 11.7°. Also shown is a shock-free design that is derived from this wing that has somewhat less thickness. Figure 5 provides the same results for a wing that is the result of our shock-free wing design procedure. Here we have taken a baseline that is about .3% thicker than that desired. The designed wing has a lift coefficient of 0.439 at M_∞ = 0.80 and is 11.7° thick. The relative changes in the section drag coefficients are indicative of the inviscid improvement in the drag, but the individual magnitudes are obviously wrong. For the shock-free design the boundary layer will obviously not separate, but this is much less likely for the wing with the GAW)-2T section. While these results are given for invisicid flow, they have been repeated with the section boundary-layer displacement thickness that, when used with the inviscid algorithm FLO6, gives essentially the same results as the GRUMFOIL algorithm. Further improvemnts are no doubt possible, but these should serve to illustrate the effectiveness of the fictitious gas design method.

The design process in the presence of inviscid - viscous interactions that was successful in two dimensions is, as one would expect, also successful in three dimensions. We have used the algorithm developed by Stock (16) at Dornier for three-dimensional boundary layer calcuations to provide the boundary layer displacement surface for the FLO22 computations. The two codes are interfaced with the PABLIM algorithm of C. L. Streett (private communication). Figure 6 shows the pressures on the original baseline wing used in the above study with those found on the wing designed to be shock free at M_∞ = 0.76 for a Reynolds number of $6 \cdot 10^6$. We are now in the process of repeating our inviscid design study to find an equivalent design when invisicd - viscous interactions are included.

CONCLUSION

It is clear that the fictitious gas method is capable of providing both airfoils and wings that are shock free. An experienced practioner can push these designs to the natural barrier that seems to limit the maximum Mach number for fixed lift, or the maximum lift for fixed Mach number, for which shock-free designs are possible. Such studies can also be carried out successfully in the presence of viscous - inviscid interactions. Thus, the method can be used to provide very slight modifications to an already suitable design to maximize M_∞ L/D. We note that while a shock-free design point does not maximize this quantity, a shock-free design need only be used at a very slightly higher Mach number to achieve what must be near to the maximum possible for a given lift, Mach number, and thickness.

Acknowledgement

The authors are indebted to the Air Force Office of Scientific Research and the Office of Naval Research for their support of this research. They are also indebted to the NASA Ames Research Center for remote access to their CDC 7600 and for an allocation of computer resources for this and other studies related to NASA's support of the University of Arizona's CFD Traineeships. They wish to thank C. L. Streett for supplying his PABLIM algorithm for this study and Mr. Leopold of the DFVLR in Gottingen for the graphics for Figure 6.

REFERENCES

[1] Nieuwland, G. Y., "Transonic Potential Flow around a Family of Quasi-elliptical Airfoil Sections," National Aerospace Laboratory, The Netherlands, TR-T172, 1967.

[2] Bauer, F., Garabedian, P., and Korn, D., "Supercritical Wing Sections III," Lecture Notes in Economics and Mathematical Systems, No. 108, Springer, New York 1975.

[3] Sobieczky, H., "Entwurf überkrittscher Profile mit Hilfe der rheoelektrischen Analogie," Deutsche Forschungs-und Versuchsanstalt fur Luft-und Raumfahrt Report DLR-75-43, 1977.

[4] Sobieczky, H., "Die Berechnung lokaler räumlicher Uberschallfelder," ZAMM, 58T, 1978.

[5] Sobieczky, H., Yu, N. J., Fung, K.-Y., and Seebass, A. R., "New Method for Designing Shock-Free Transonic Configurations," AIAA J., Vol. 17, No. 7, pp. 722-729, 1979.

[6] Fung, K.-Y., Sobieczky, H., and Seebass, R., "Shock-Free Wing Design," AIAA J., Vol. 18, No. 10, pp. 1153-1158, 1980.

[7] Lynch, F. T., "Commercial Transports-Aerodynamic Design for Cruise Performance and Efficiency," Douglas Aircraft Company Paper 7026, 1981.

[8] McGhee, R. J., Beasley, W. D., and Somers, D. M., "Low-Speed Aerodynamic Characteristics of a 13-Percent-Thick Airfoil Section Designed for General Aviation Applications," NASA TM X-72697, 1975.

[9] Melnik, R. E., "Turbulent Interactions on Airfoils at Transonic Speeds--Recent Developments," Computation of Viscous-Inviscid Interactions, AGARD CP No. 291, 1981.

[10] Nebeck, H. E. and Seebass, A. R., "Inviscid-Viscous Interactions in the Nearly Direct Design of Shock-Free Supercritical Airfoils," Computation of Viscous-Inviscid Interactions, AGARD CP No. 291, 1981

[11] Sobieczky, H., "Computational Algorithms for Wing Geometry Generation, Transonic Analysis and Design," University of Arizona Engineering Experiment Station, Transonic Fluid Dynamics Report TFD 80-01, 1980.

[12] Jameson, A. and Caughey, D. A., "Numerical Calculations of the Transonic Flow Past a Swept Wing," NASA CR-153297, 1977.

[13] Yu, N. J., "An Efficient Transonic Shock-Free Wing Redesign Procedure using a Fictitious Gas Method," AIAA J., Vol. 18, No. 2, pp. 143-148, 1980.

[14] Raj, P., Miranda, L. R., Seebass, A. R., "A Cost-Effective Method for Shock-Free Supercritical Wing Design," AIAA Paper 81-0383, AIAA 19th Aerospace Sciences Meeting, St. Louis, January 1981.

[15] Henne, P. A., "Inverse Transonic Wing Design Method," J. Aircraft, Vol. 18, No. 2, pp. 121-127, 1981.

[16] Stock, H. W., "Integral Method for the Calculation of Three-Dimensional Laminar and Turbulent Boundary Layers," (translation of Dornier Report), NASA TM 75320, 1978.

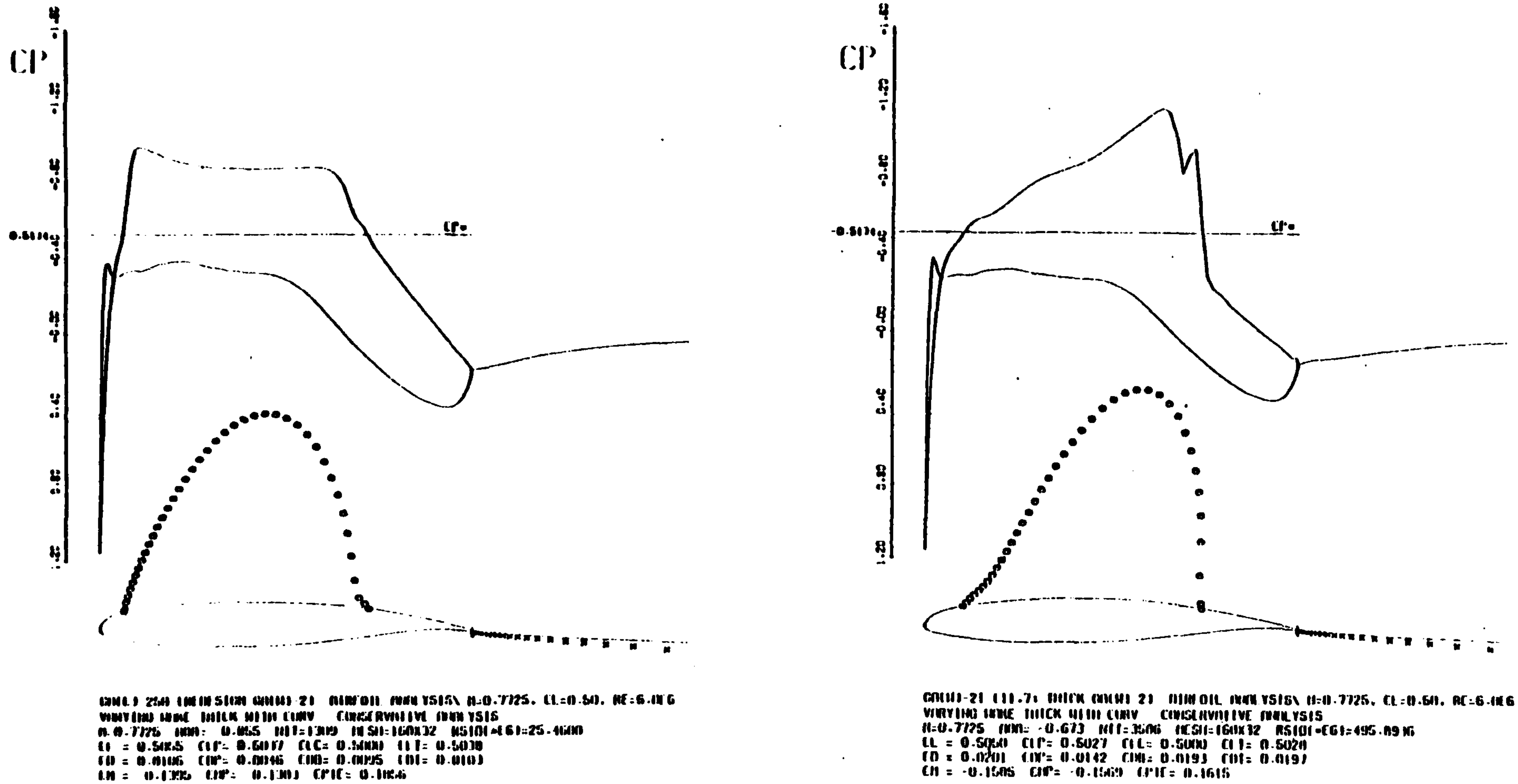

Figure 1. Comparison on the pressures and sonic line shapes on the GA(C)-250 and GA(W)-2T airfoils at $M_\infty = 0.7725$, $C_L = 0.50$, and $Re = 6 \cdot 10^6$.

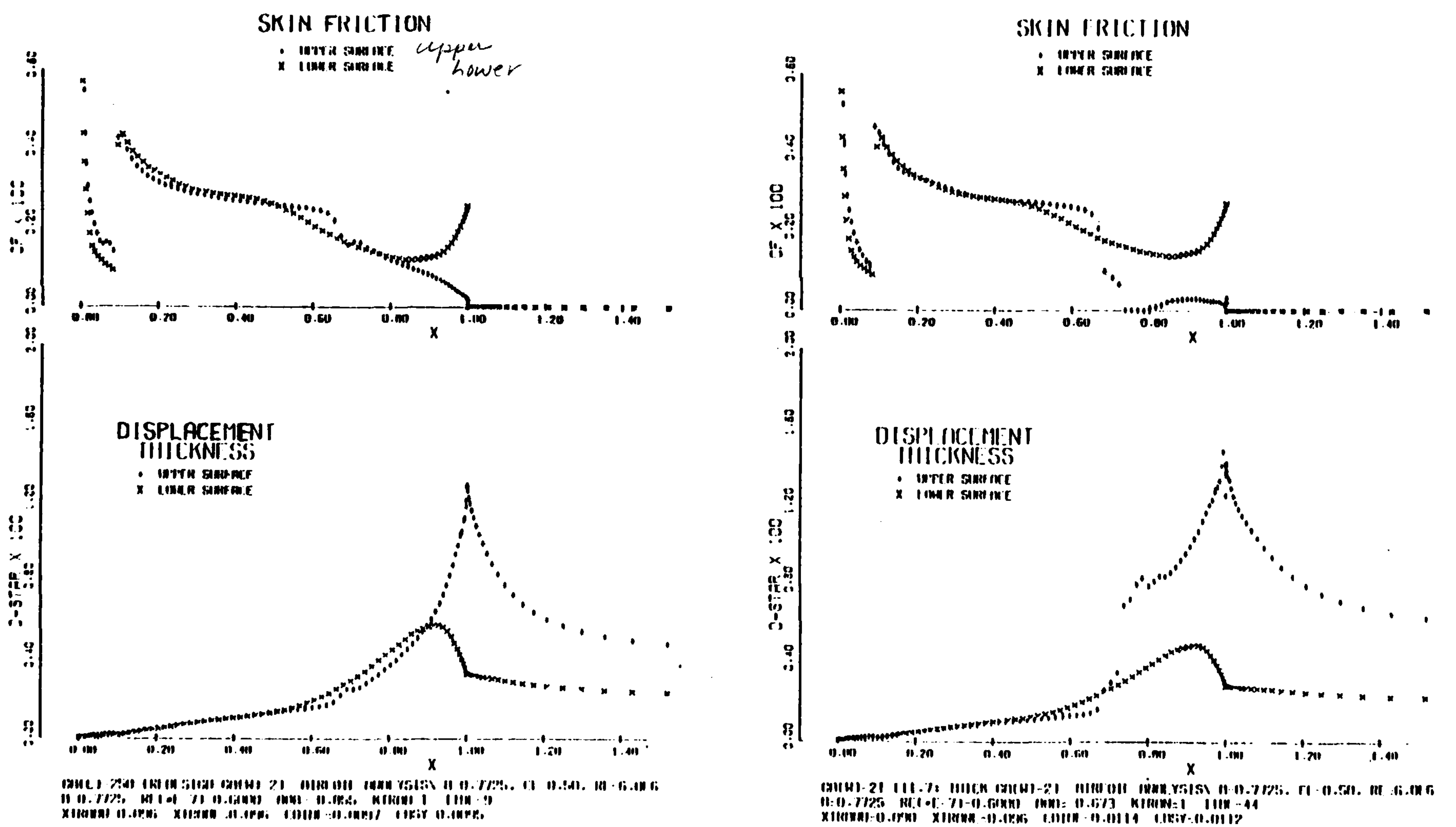

Figure 2. Skin friction and boundary-layer displacement thickness on the GA(C)-250 and GA(W)-2T airfoils at $M_\infty = 0.7725$, $C_L = 0.50$, and $Re = 6 \cdot 10^6$.

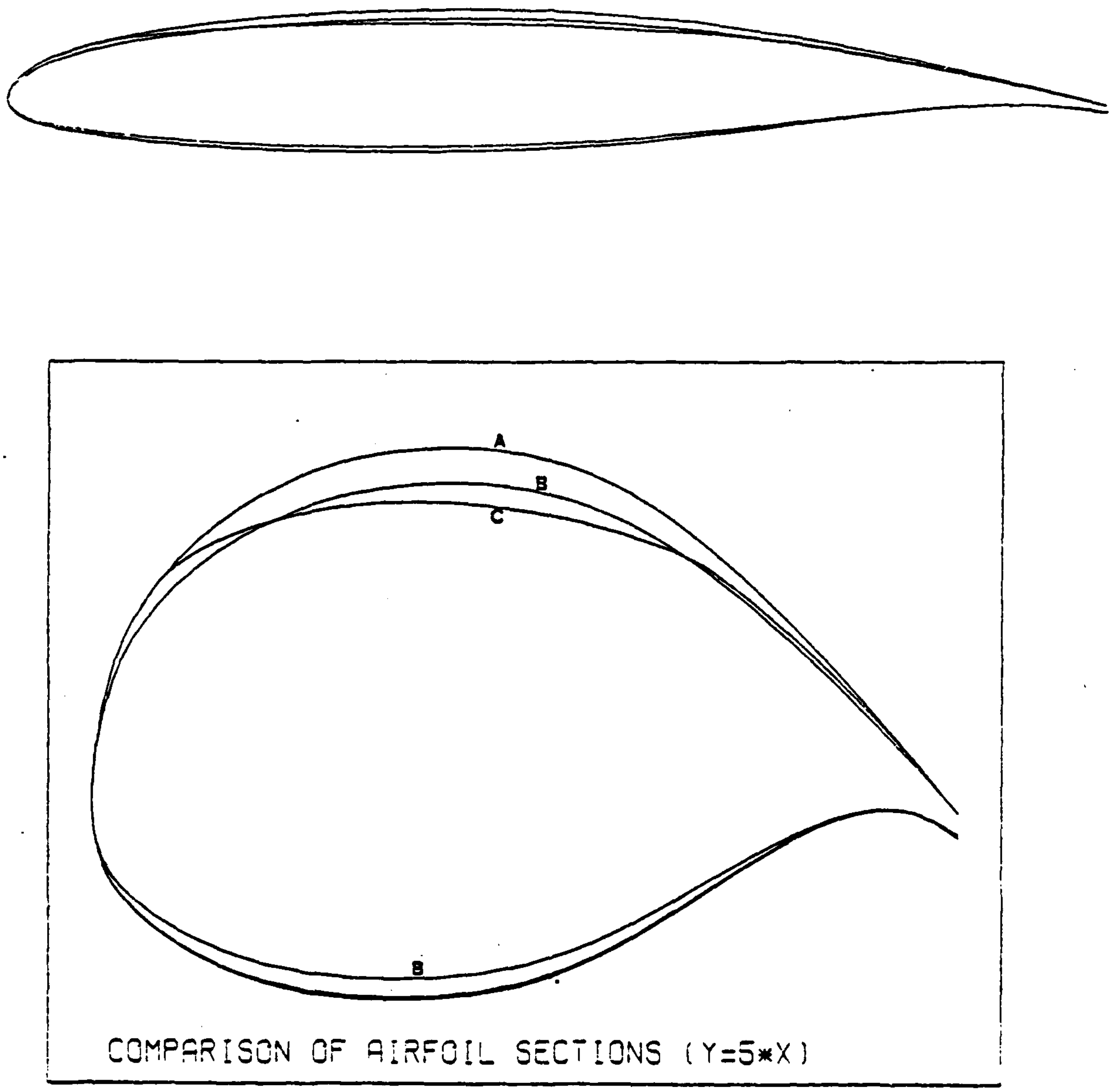

Figure 3. Comparison of the GA(W)-2 [A], GA(W)-2T [B], and GA(C)-250 [C] airfoils.

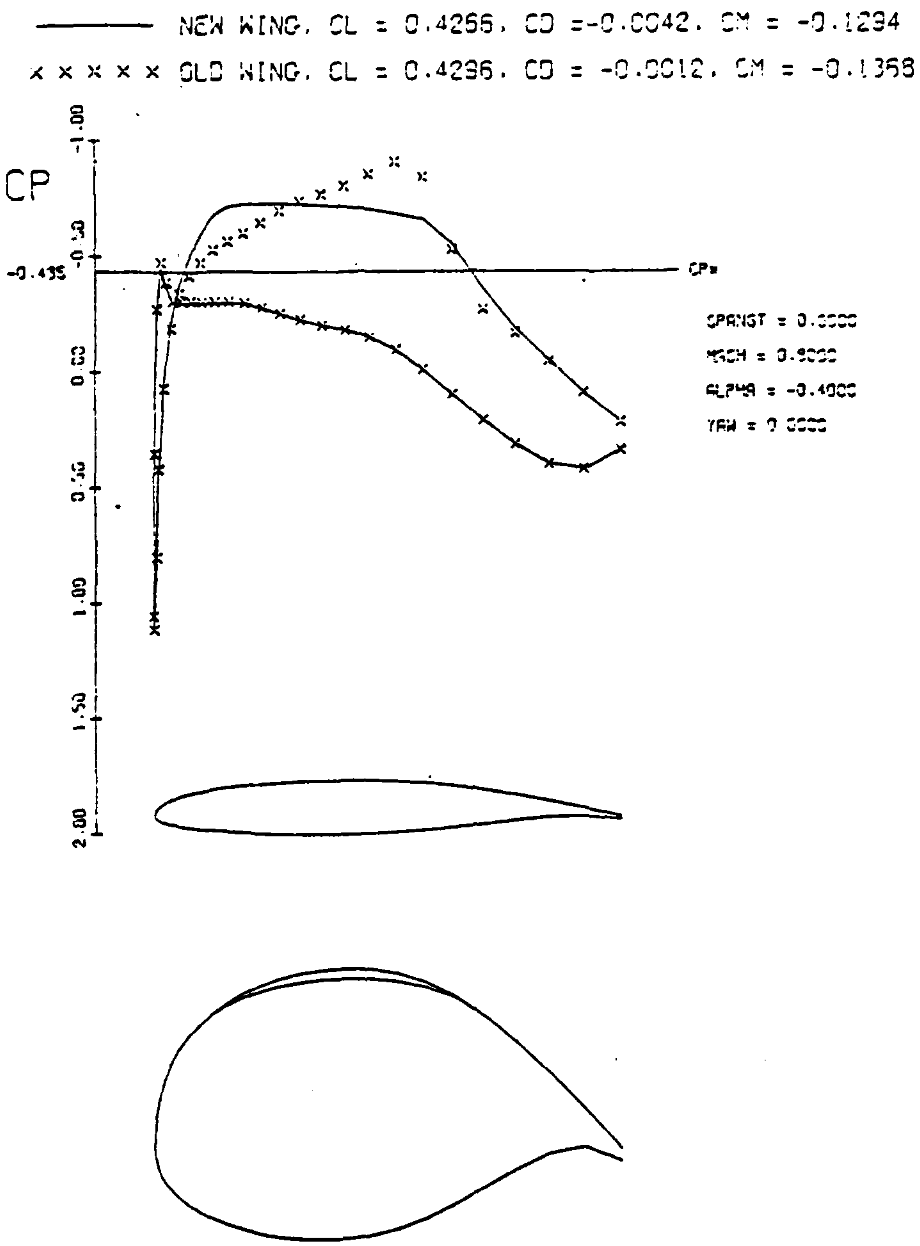

Figure 4. Pressures and wing section shapes for a wing derived from the GA(W)-2T airfoil and a shock-free design that results from this airfoil when used as a basaline. The lift coeficient of the non-shock free wing is 0.430 and the wing root is 11.7 per cent thick. The lift coefficient for the shock-free wing is 0.364 and this wing is about 11.4 per cent thick. The wing planform is shown at the end of the Figure.

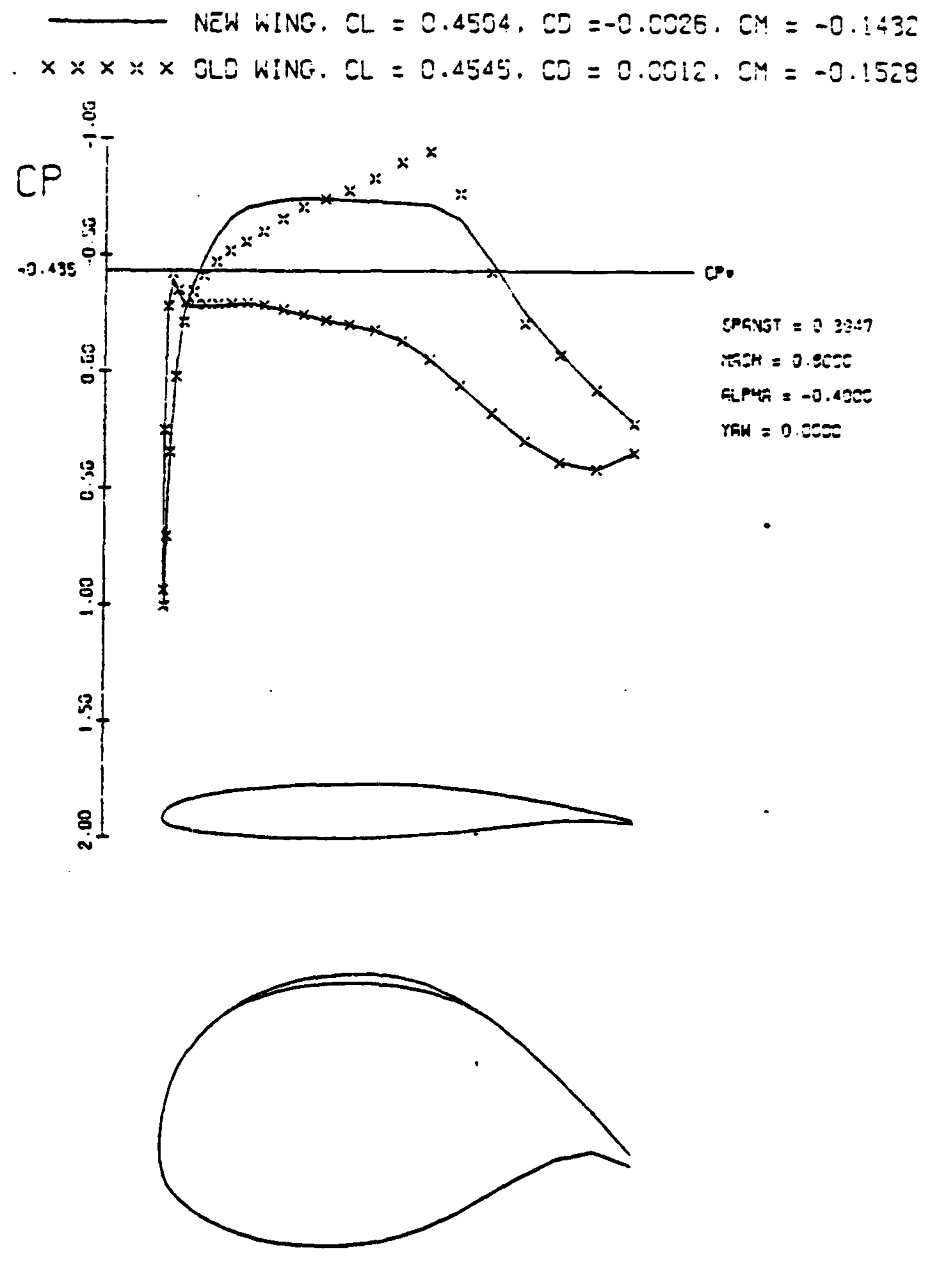

Figure 4. Pressures and wing section shapes for a wing derived from the GA(W)-2T airfoil and a shock-free design that results from this airfoil when used as a baseline. The lift coeficient of the non-shock free wing is 0.430 and the wing root is 11.7 per cent thick. The lift coefficient for the shock-free wing is 0.364 and this wing is about 11.4 per cent thick. The wing planform is shown at the end of the Figure.

Figure 4 (continued).

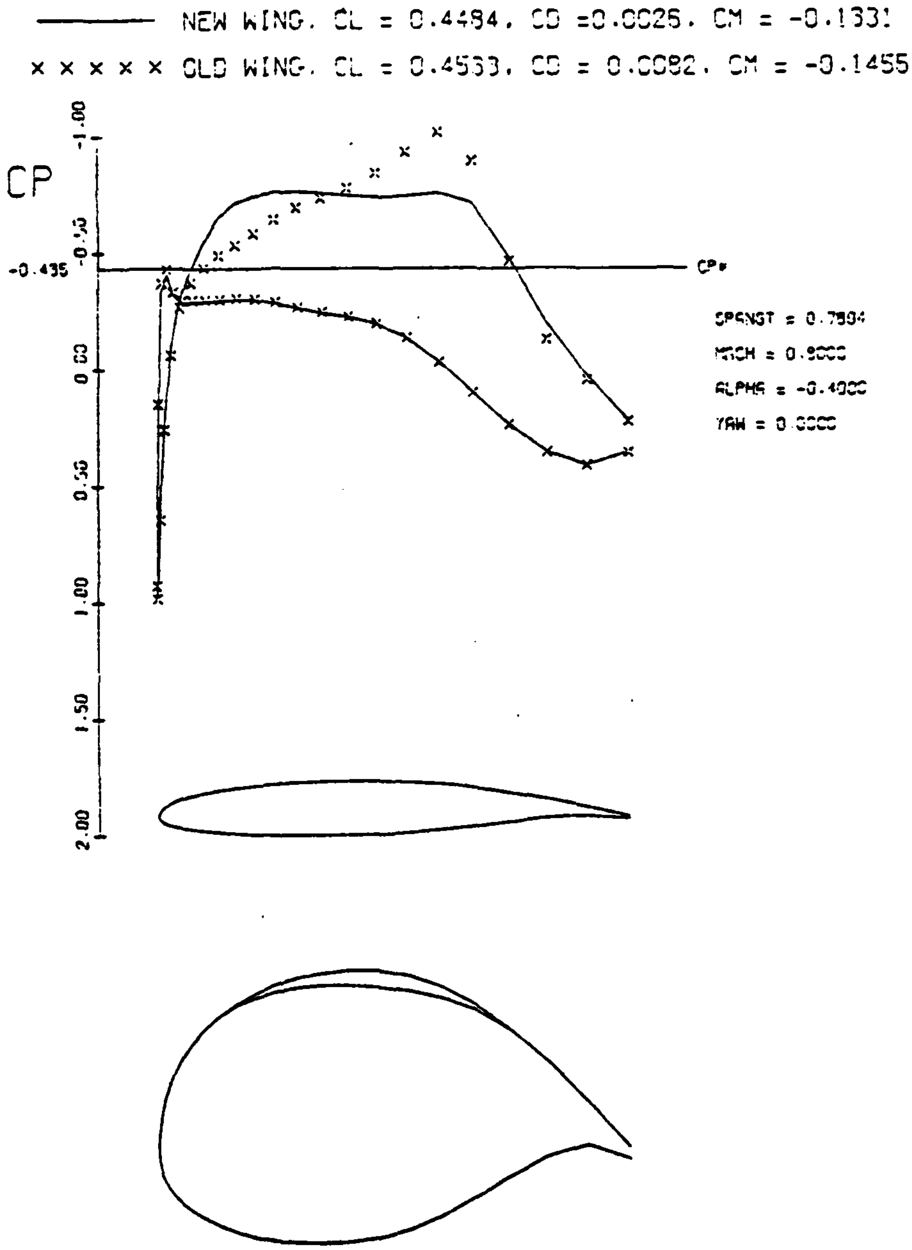

Figure 4. Pressures and wing section shapes for a wing derived from the GA(W)-2T airfoil and a shock-free design that results from this airfoil when used as a baseline. The lift coeficient of the non-shock free wing is 0.430 and the wing root is 11.7 per cent thick. The lift coefficient for the shock-free wing is 0.364 and this wing is about 11.4 per cent thick. The wing planform is shown at the end of the Figure.

Figure 4 (continued).

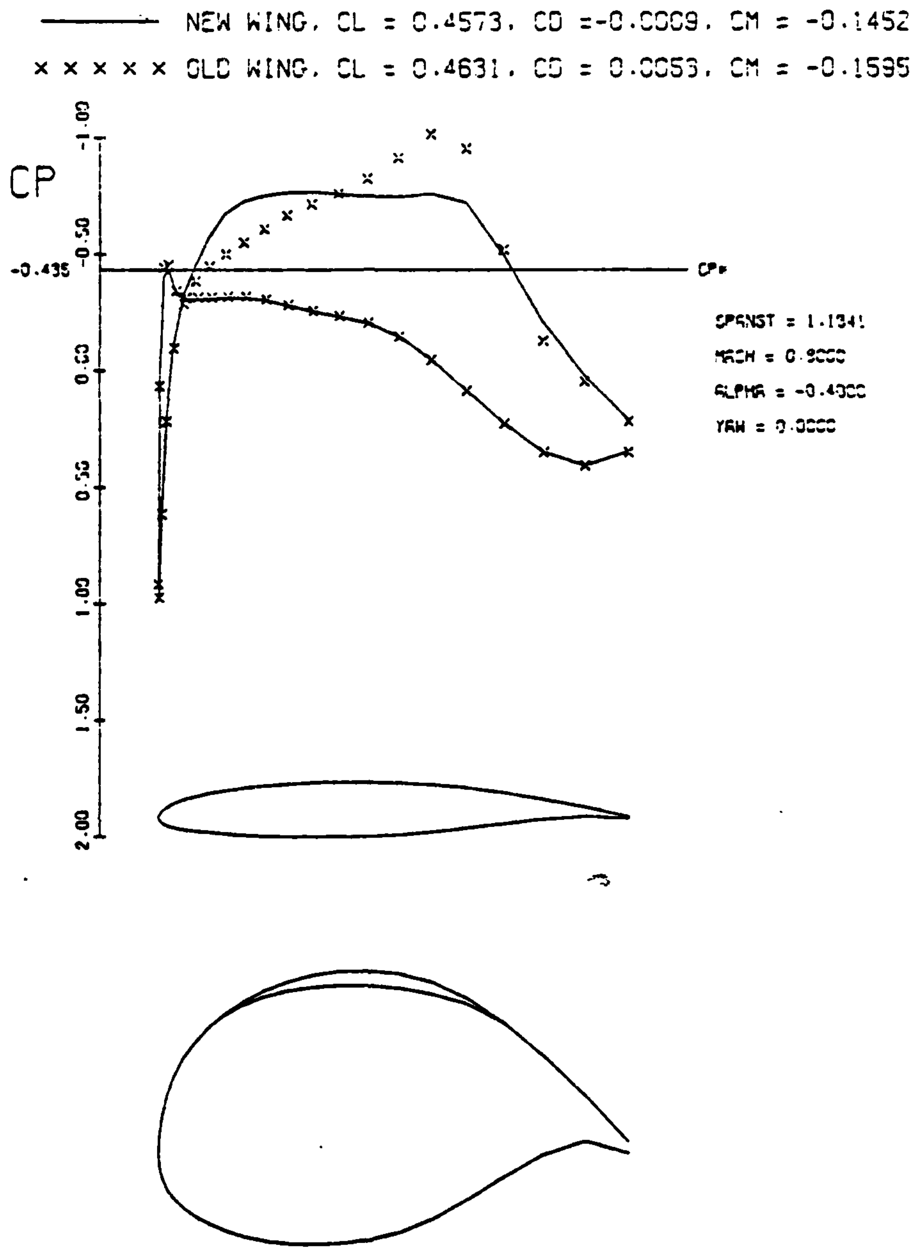

Figure 4. Pressures and wing section shapes for a wing derived from the GA(W)-2T airfoil and a shock-free design that results from this airfoil when used as a baseline. The lift coeficient of the non-shock free wing is 0.430 and the wing root is 11.7 per cent thick. The lift coefficient for the shock-free wing is 0.364 and this wing is about 11.4 per cent thick. The wing planform is shown at the end of the Figure.

Figure 4 (continued).

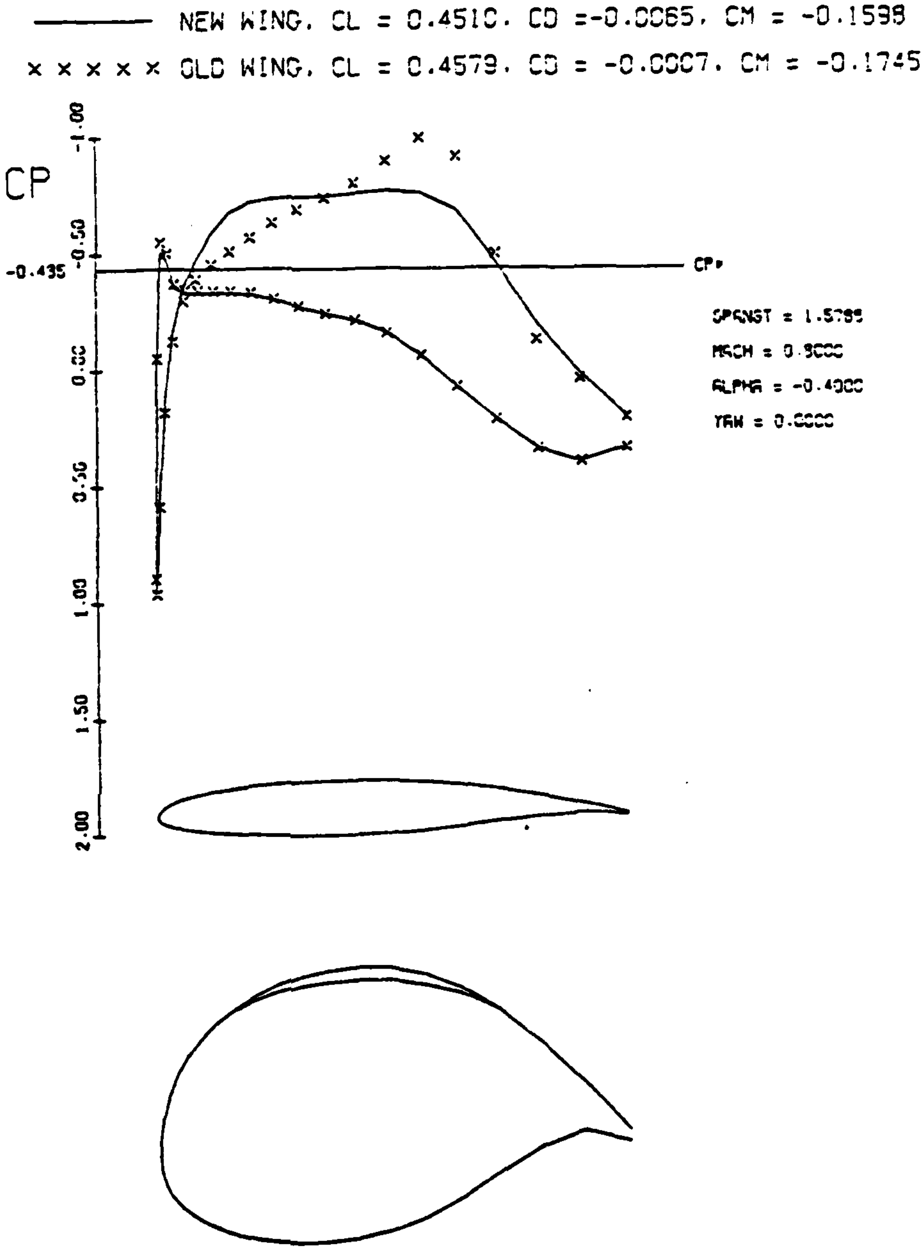

Figure 4. Pressures and wing section shapes for a wing derived from the GA(W)-2T airfoil and a shock-free design that results from this airfoil when used as a baseline. The lift coeficient of the non-shock free wing is 0.430 and the wing root is 11.7 per cent thick. The lift coefficient for the shock-free wing is 0.364 and this wing is about 11.4 per cent thick. The wing planform is shown at the end of the Figure.

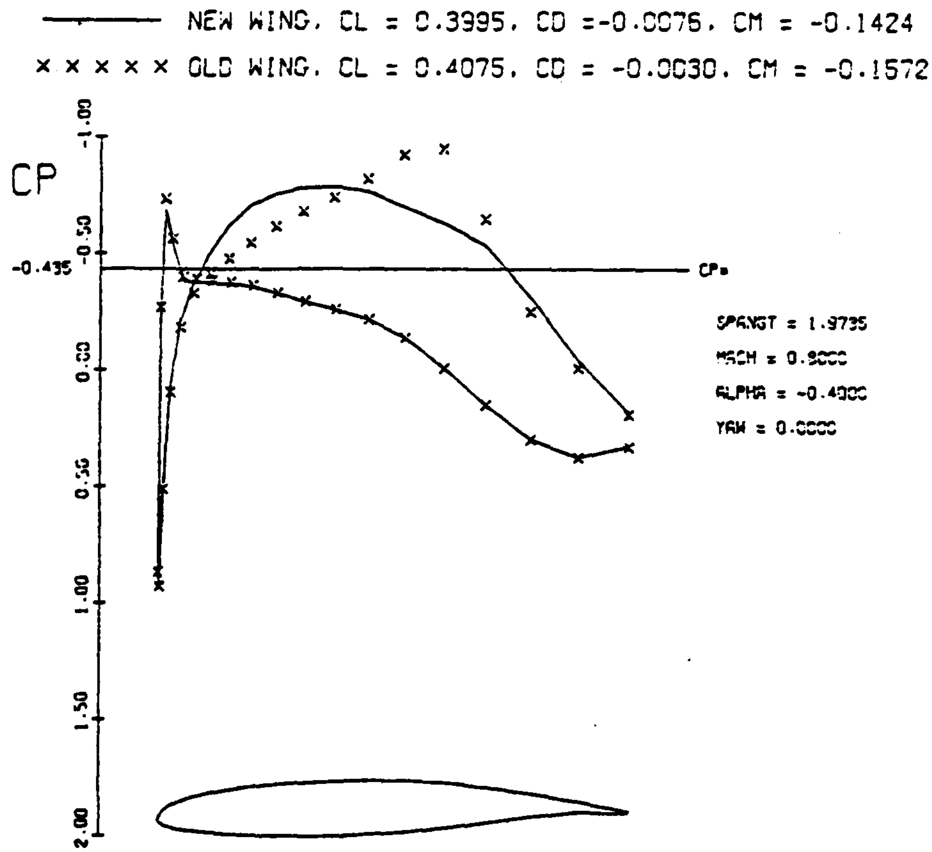

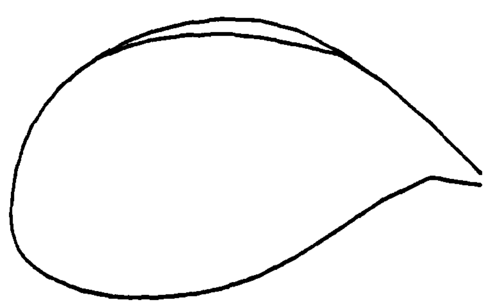

Figure 4. Pressures and wing section shapes for a wing derived from the GA(W)-2T airfoil and a shock-free design that results from this airfoil when used as a baseline. The lift coeficient of the non-shock free wing is 0.430 and the wing root is 11.7 per cent thick. The lift coefficient for the shock-free wing is 0.364 and this wing is about 11.4 per cent thick. The wing planform is shown at the end of the Figure.

Figure 4 (continued).

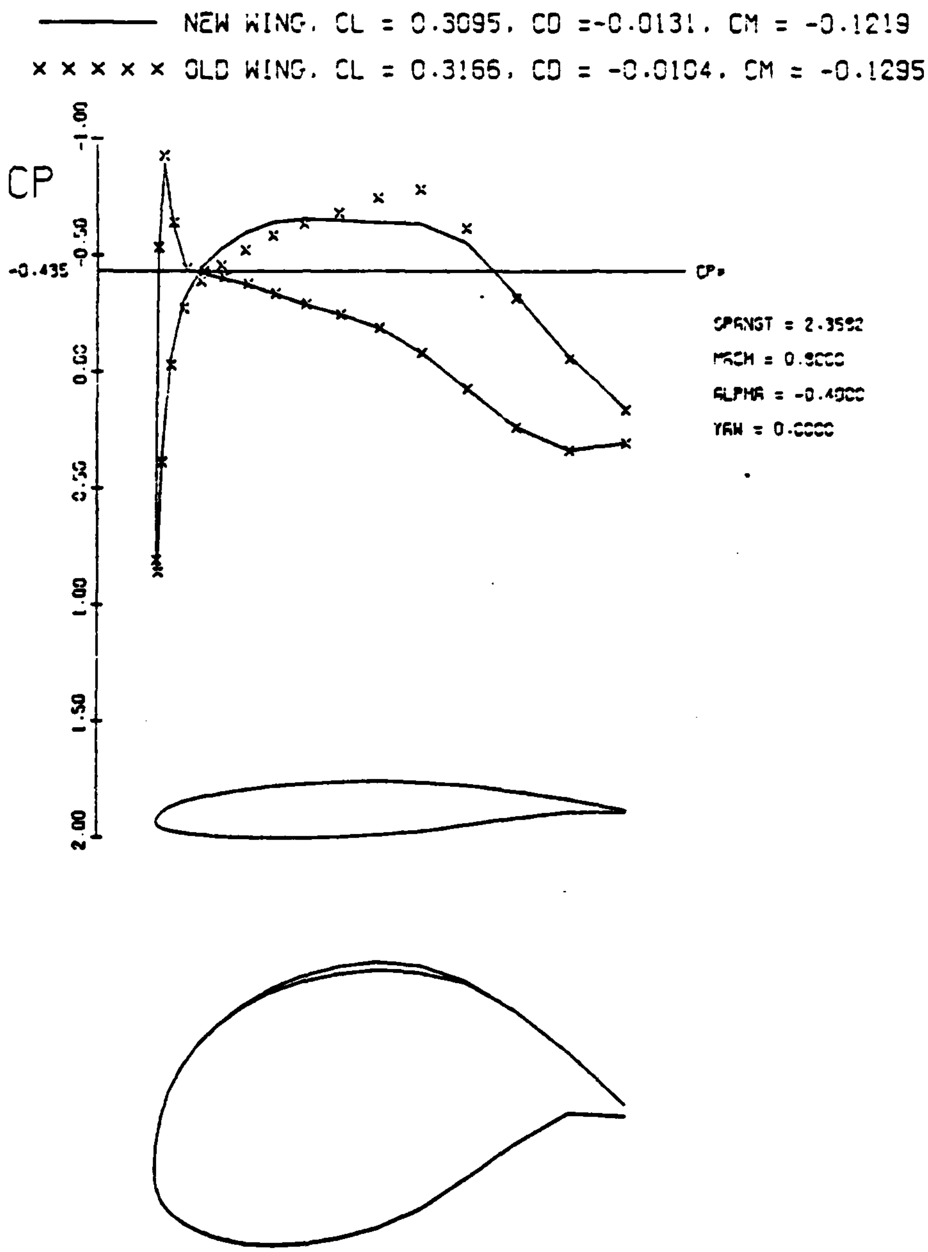

Figure 4. Pressures and wing section shapes for a wing derived from the GA(W)-2T airfoil and a shock-free design that results from this airfoil when used as a baseline. The lift coeficient of the non-shock free wing is 0.430 and the wing root is 11.7 per cent thick. The lift coefficient for the shock-free wing is 0.364 and this wing is about 11.4 per cent thick. The wing planform is shown at the end of the Figure.

Figure 4 (continued).

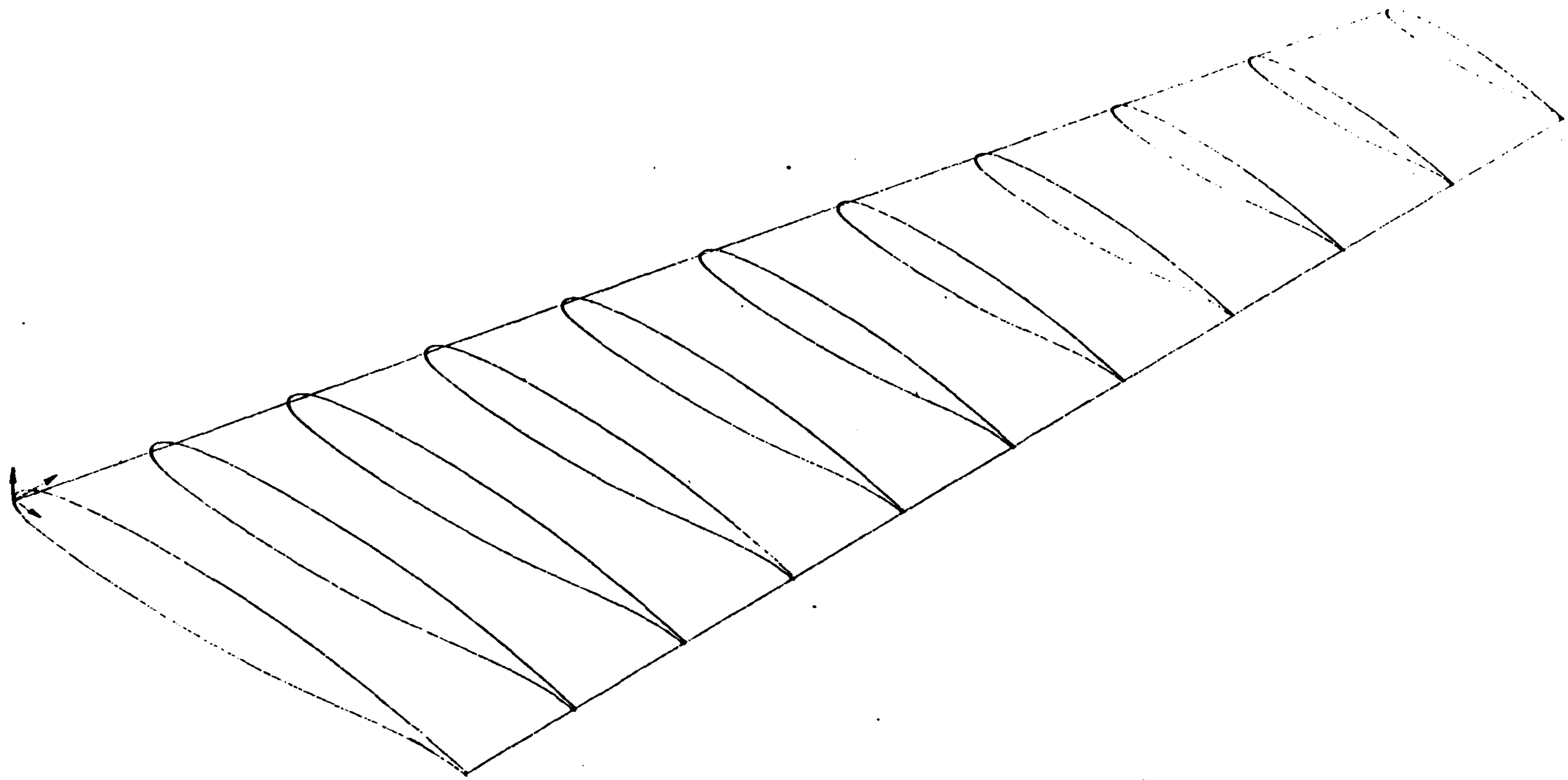

Figures 4&5. Learjet Century III wing planform with the baseline airfoil section that was used for the shock-free wing design of Figure 5.

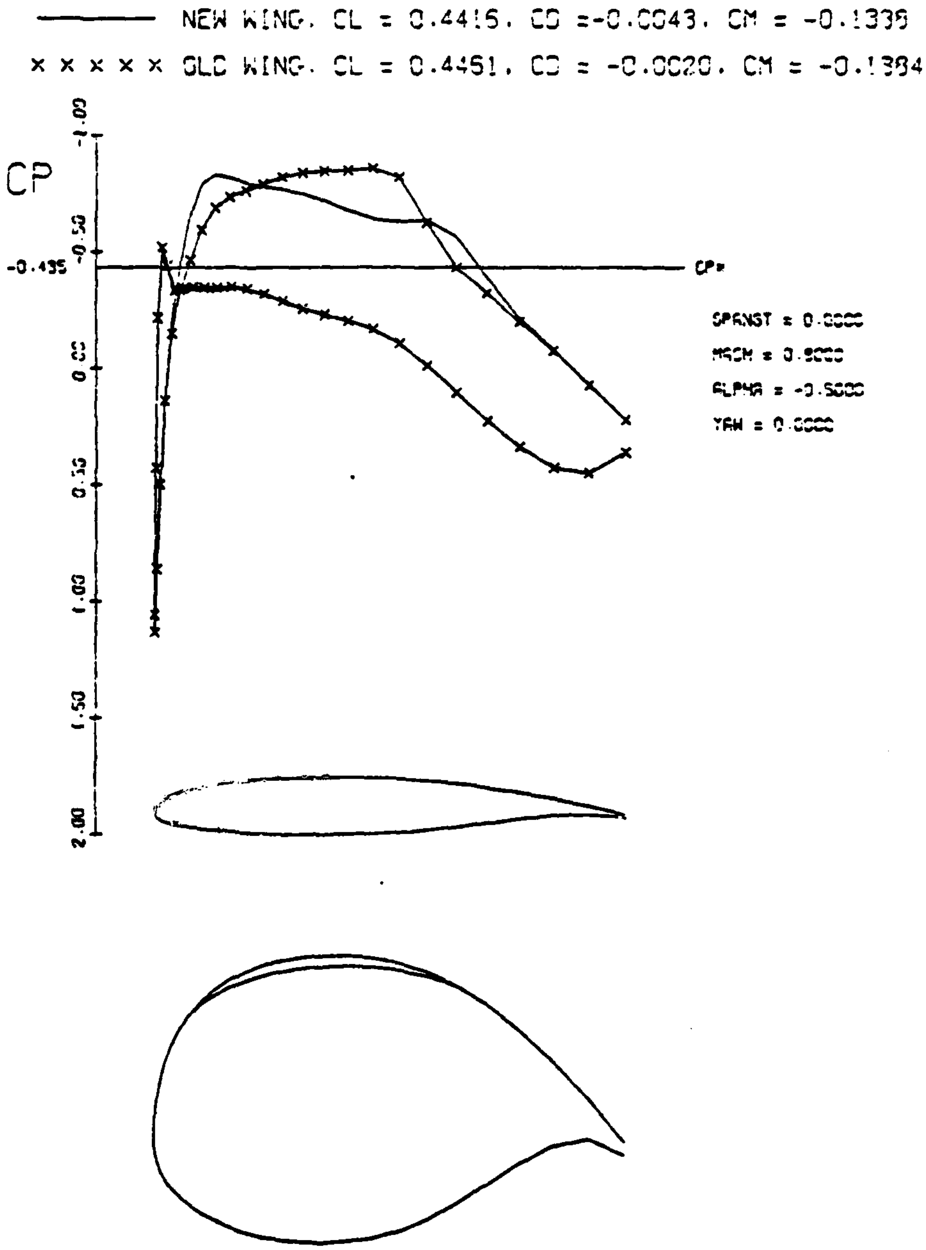

Figure 5. Pressures and wing section shapes for a a wing derived from the baseline airfoil that gave the GA(C)-250 shock-free airfoil. Also shown are the pressures on this baseline airfoil. The lift coef- ficent of the shock-free design is 0.439; that for the baseline wing is 0. 447. The proper comparison here is between this shock-free design and the old wing of Figure 4. These wings have the same thick- ness and nearly the same lift coefficient.

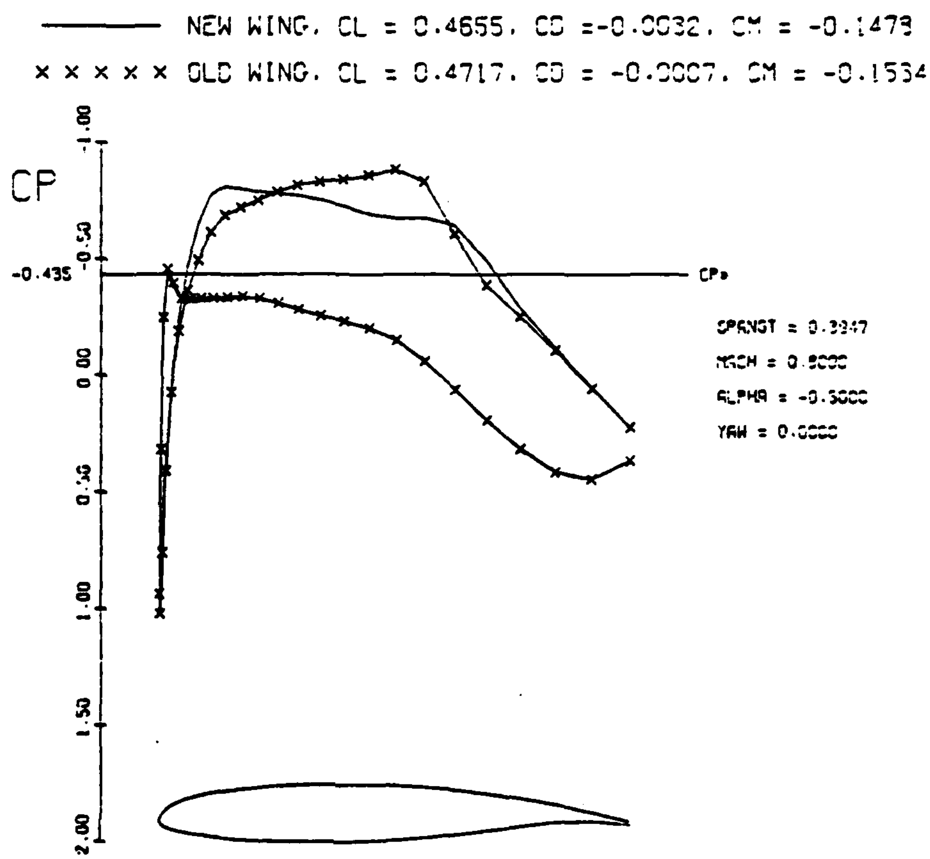

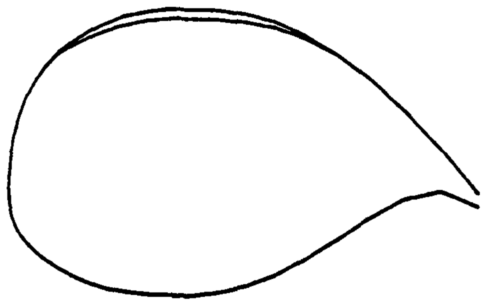

Figure 5. Pressures and wing section shapes for a a wing derived from the baseline airfoil that gave the GA(C)-250 shock-free airfoil. Also shown are the pressures on this baseline airfoil. The lift coefficent of the shock-free design is 0.439; that for the baseline wing is 0. 447. The proper comparison here is between this shock-free design and the old wing of Figure 4. These wings have the same thickness and nearly the same lift coefficient.

Figure 5 (continued).

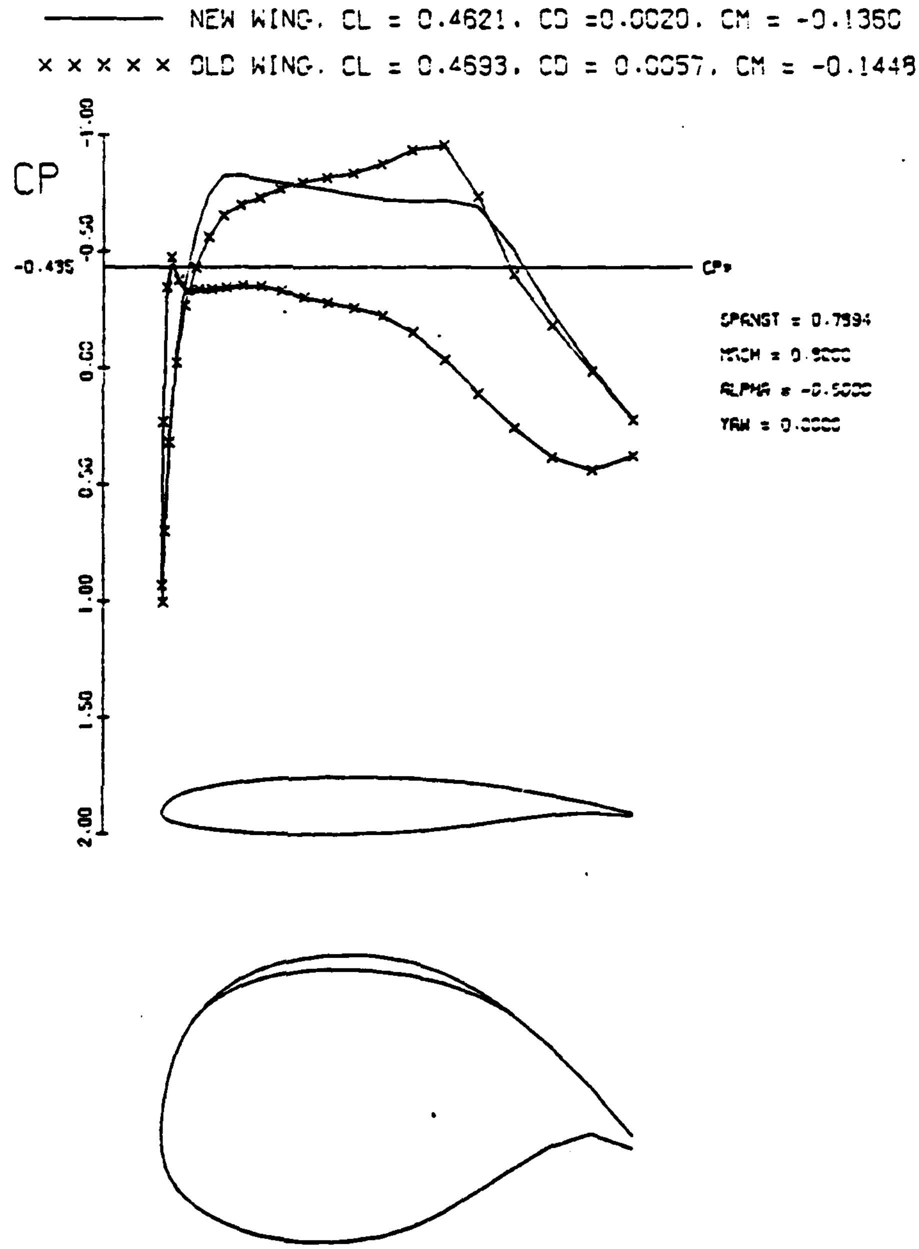

Figure 5. Pressures and wing section shapes for a a wing derived from the baseline airfoil that gave the GA(C)-250 shock-free airfoil. Also shown are the pressures on this baseline airfoil. The lift coefficient of the shock-free design is 0.439; that for the baseline wing is 0. 447. The proper comparison here is between this shock-free design and the old wing of Figure 4. These wings have the same thickness and nearly the same lift coefficient.

Figure 5 (continued).

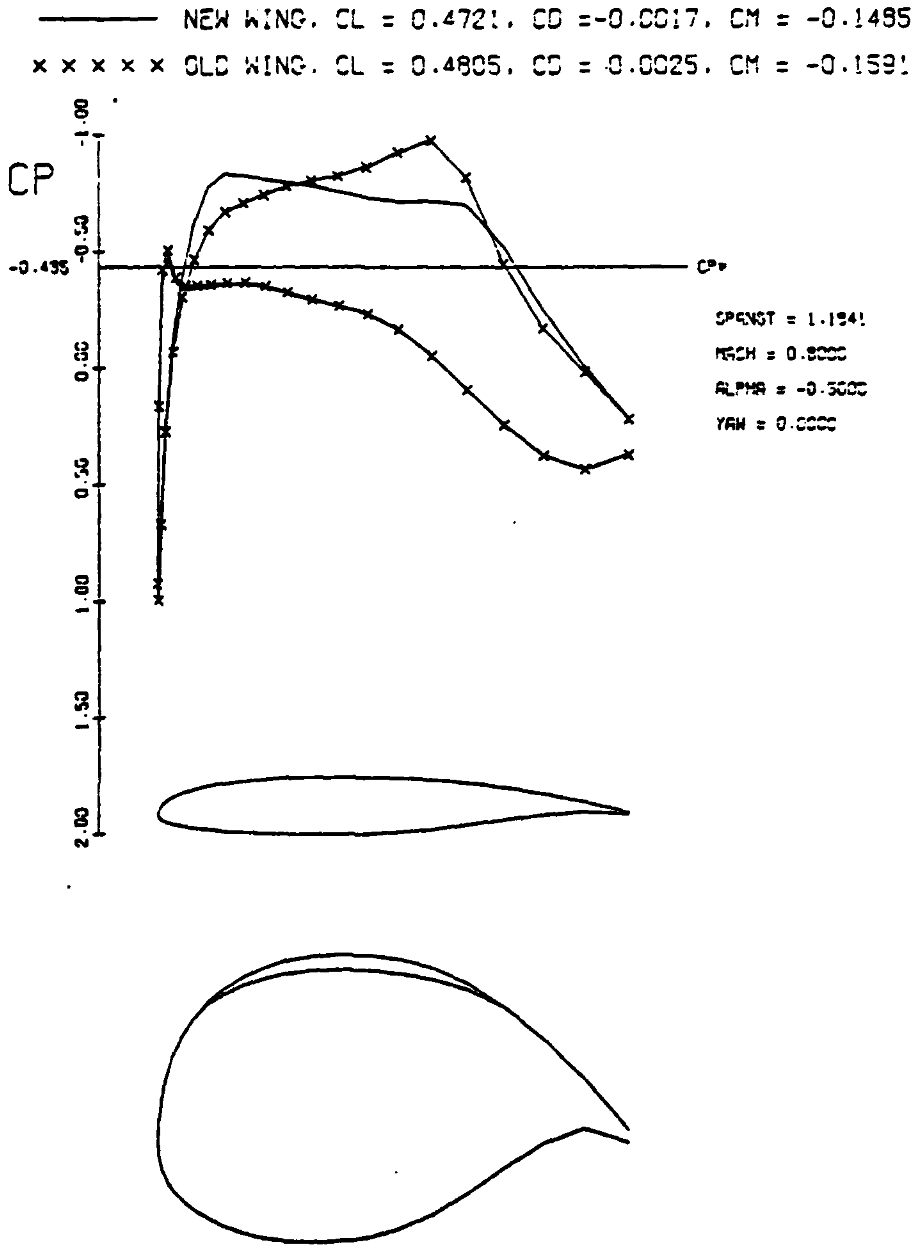

Figure 5. Pressures and wing section shapes for a a wing derived from the baseline airfoil that gave the GA(C)-250 shock-free airfoil. Also shown are the pressures on this baseline airfoil. The lift coefficient of the shock-free design is 0.439; that for the baseline wing is 0. 447. The proper comparison here is between this shock-free design and the old wing of Figure 4. These wings have the same thickness and nearly the same lift coefficient.

Figure 5 (continued).

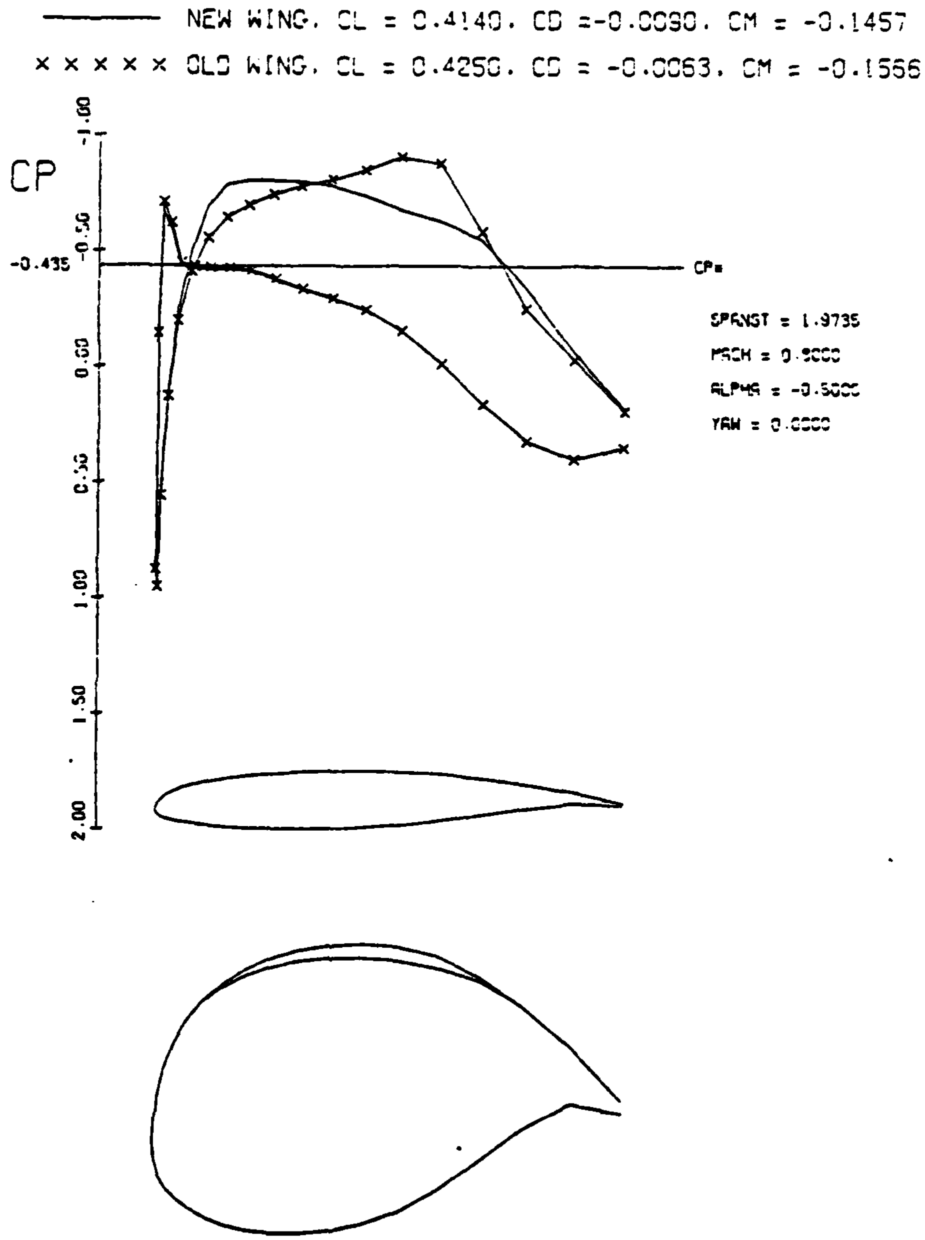

Figure 5. Pressures and wing section shapes for a a wing derived from the baseline airfoil that gave the GA(C)-250 shock-free airfoil. Also shown are the pressures on this baseline airfoil. The lift coefficent of the shock-free design is 0.439; that for the baseline wing is 0. 447. The proper comparison here is between this shock-free design and the old wing of Figure 4. These wings have the same thickness and nearly the same lift coefficient.

Figure 5 (continued).

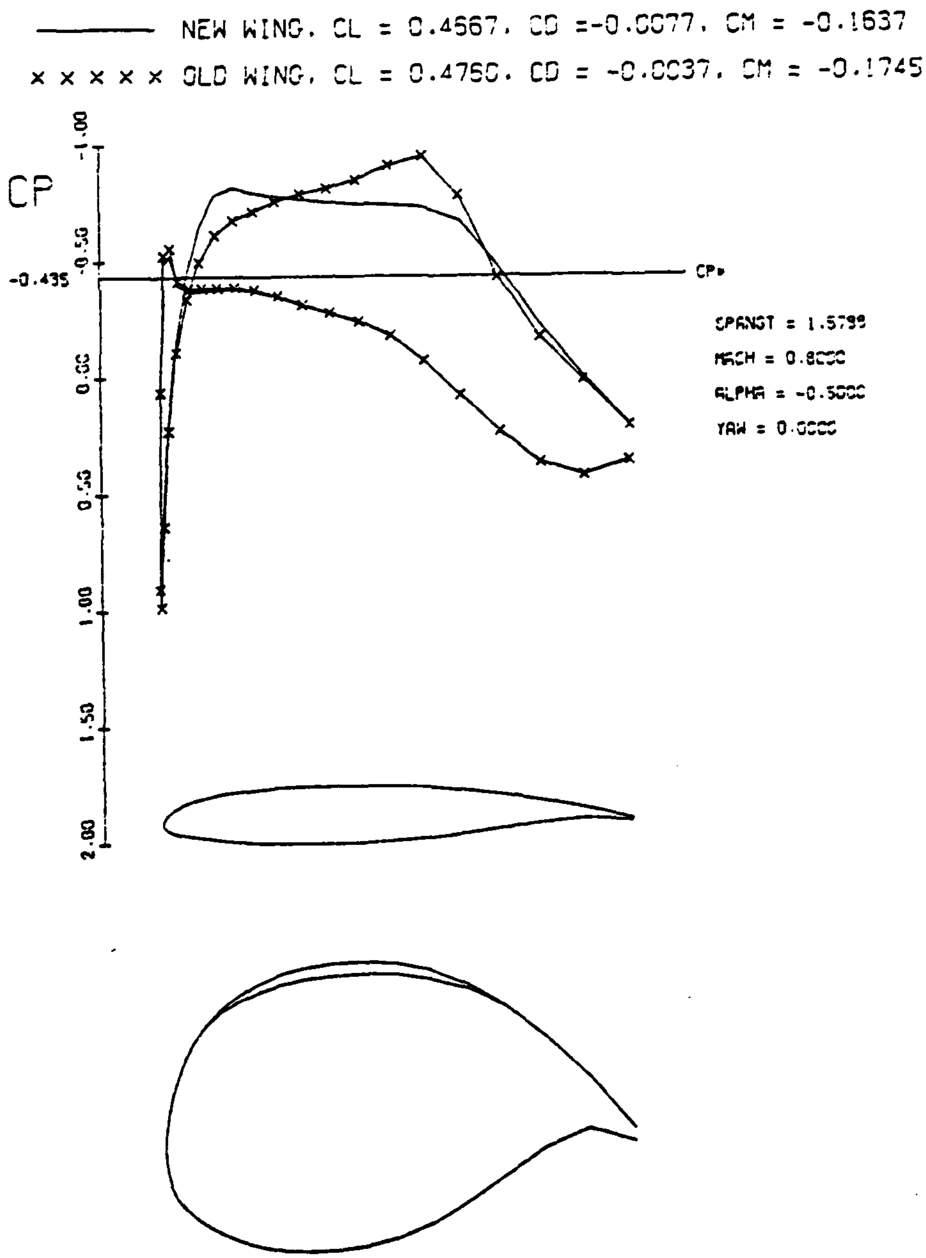

Figure 5. Pressures and wing section shapes for a a wing derived from the baseline airfoil that gave the GA(C)-250 shock-free airfoil. Also shown are the pressures on this baseline airfoil. The lift coefficient of the shock-free design is 0.439; that for the baseline wing is 0. 447. The proper comparison here is between this shock-free design and the old wing of Figure 4. These wings have the same thickness and nearly the same lift coefficient.

Figure 5 (continued).

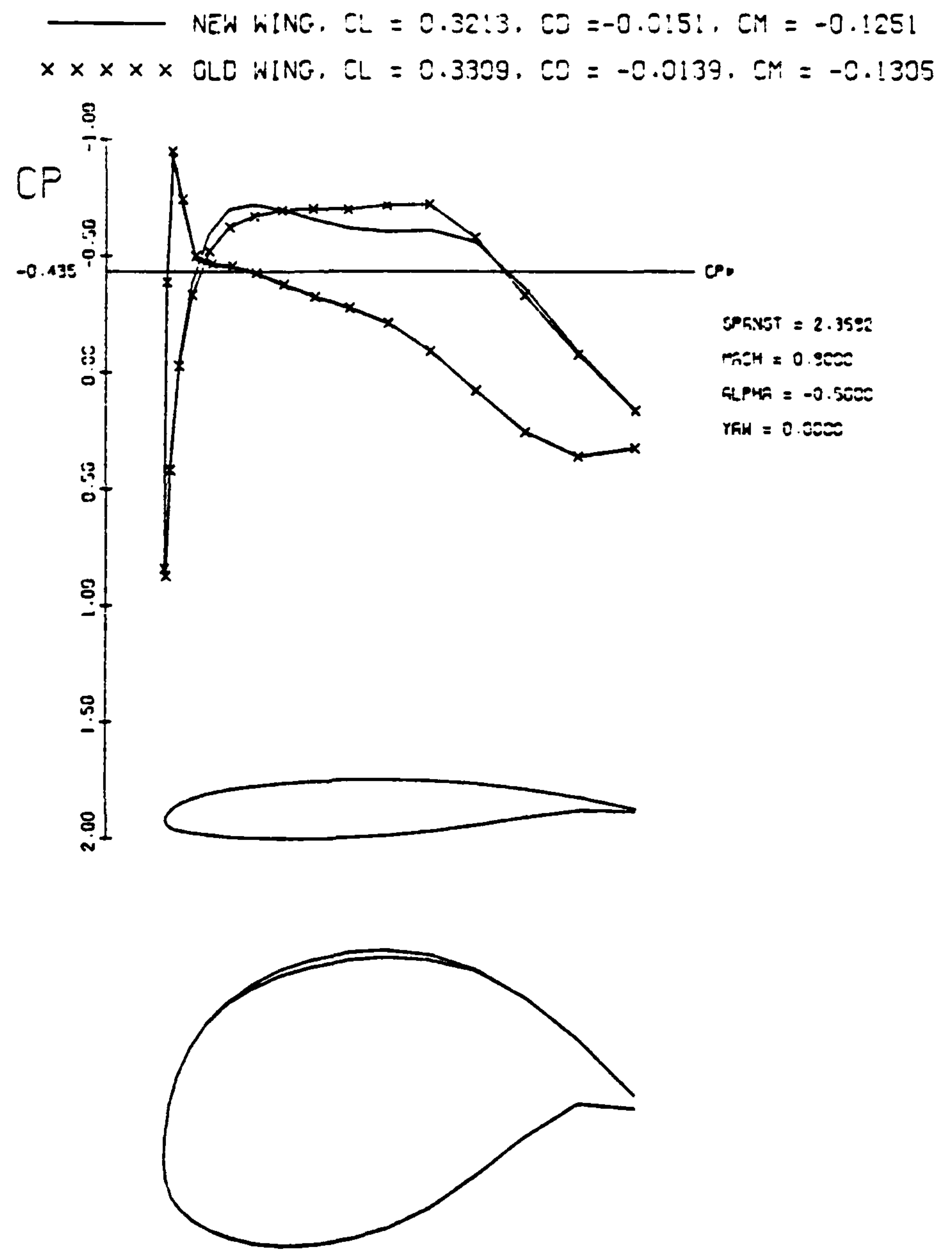

Figure 5. Pressures and wing section shapes for a a wing derived from the baseline airfoil that gave the GA(C)-250 shock-free airfoil. Also shown are the pressures on this baseline airfoil. The lift coefficent of the shock-free design is 0.439; that for the baseline wing is 0. 447. The proper comparison here is between this shock-free design and the old wing of Figure 4. These wings have the same thickness and nearly the same lift coefficient.

Figure 5 (concluded).

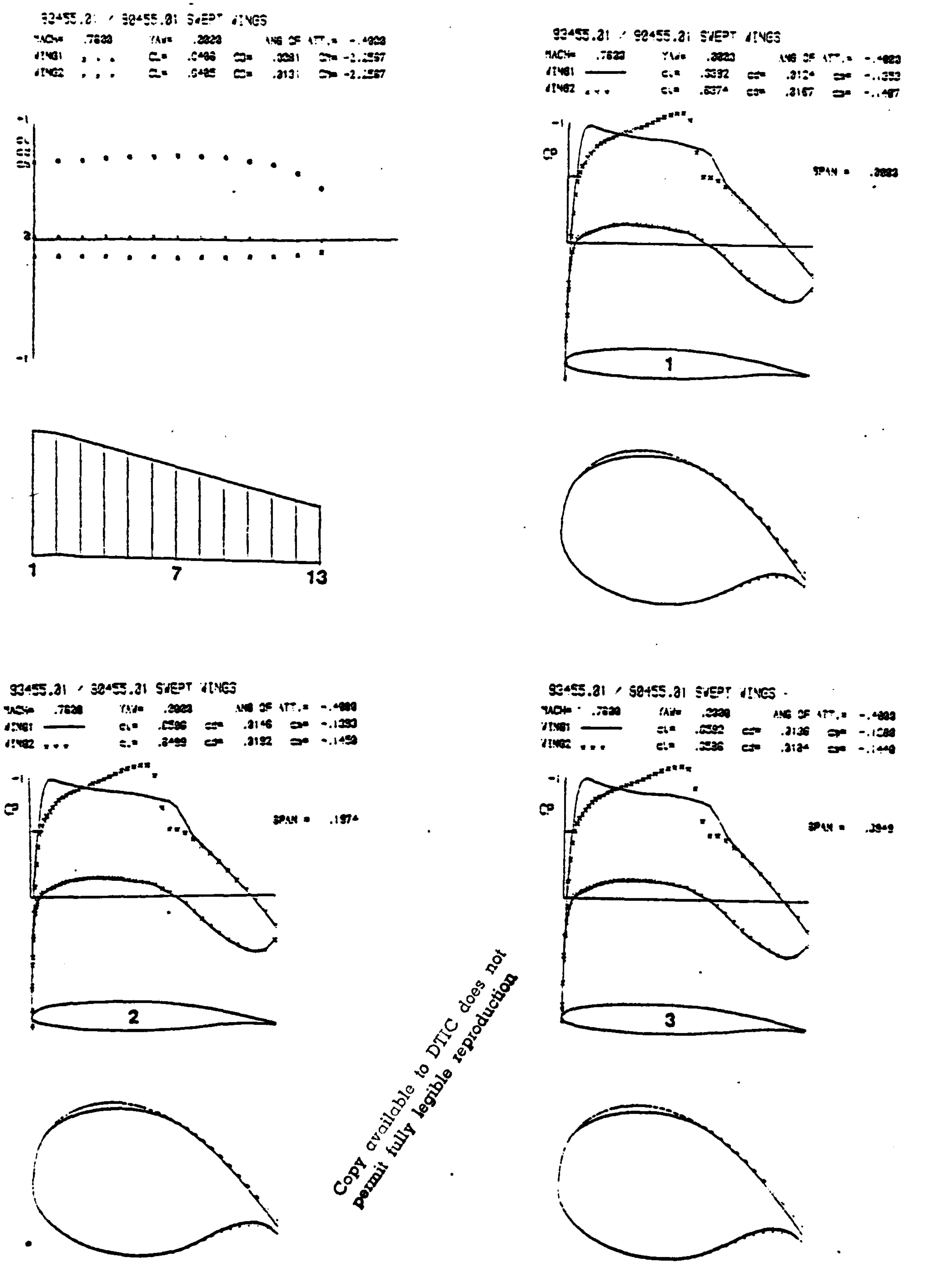

Figure 6. Wing planform, section pressures, and section shapes for a wing that was designed to be shock free in the presence of inviscid-viscous interactions using FLO22 and the Stock 3D boundary - layer algorithm coupled by Streett's BLIM algorithm.

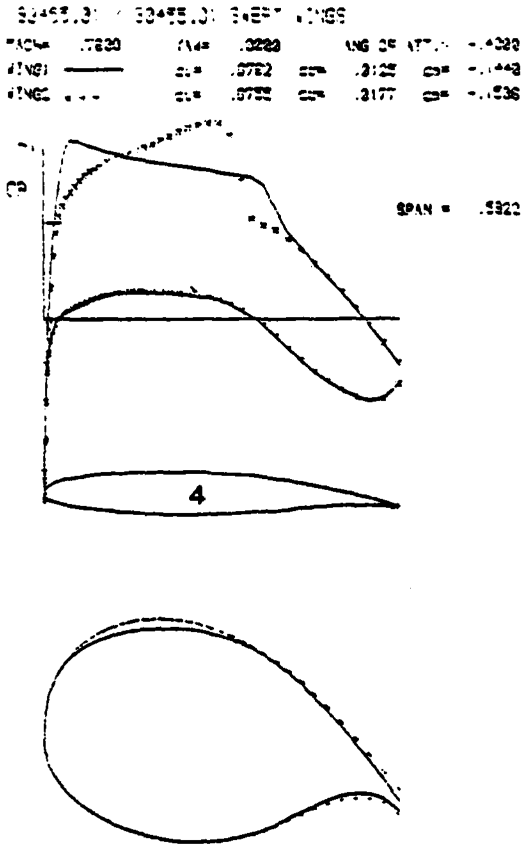

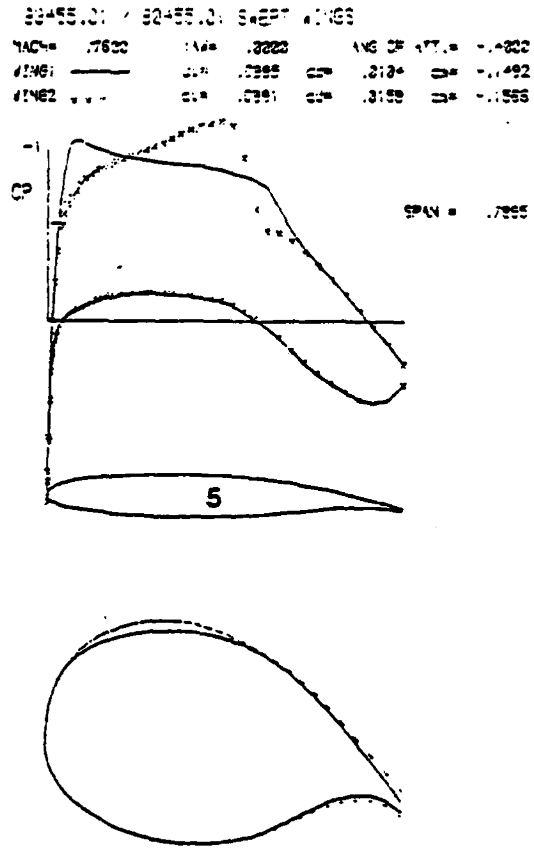

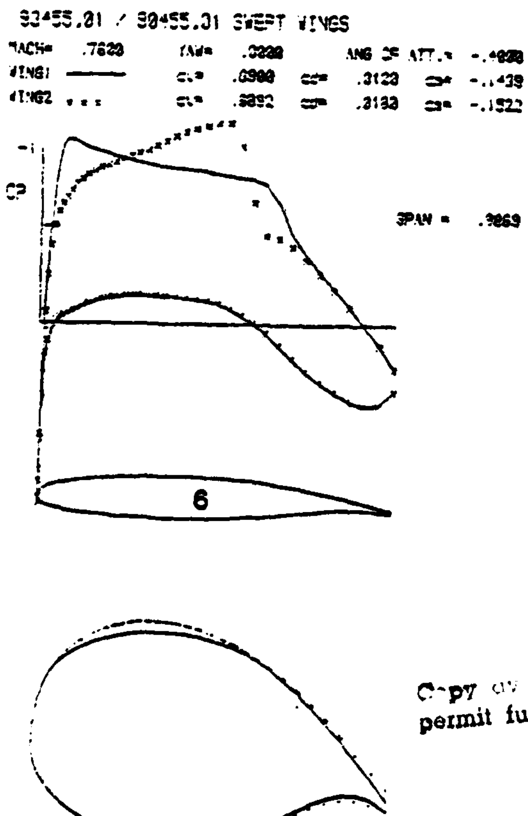

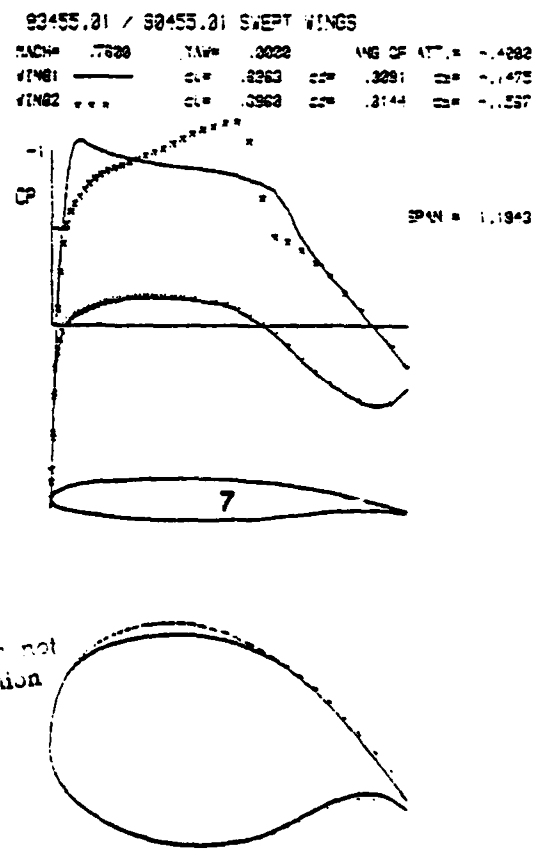

Figure 6 (continued).

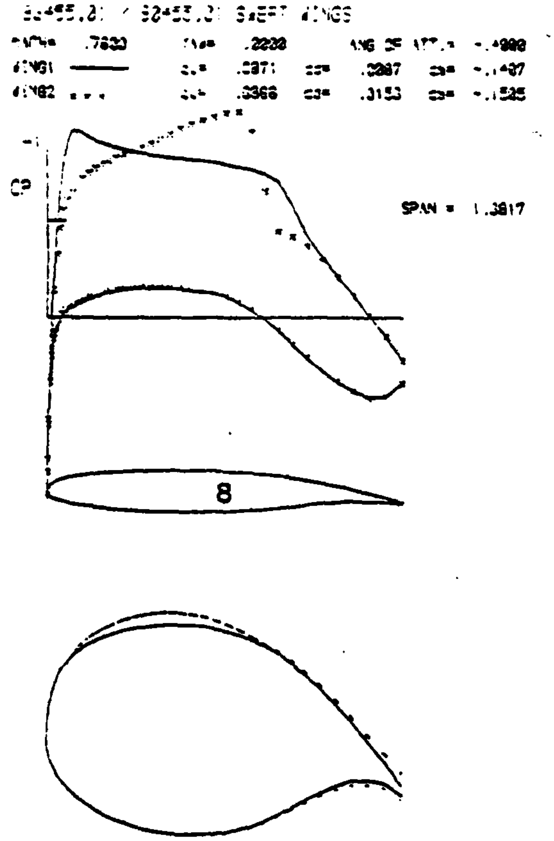

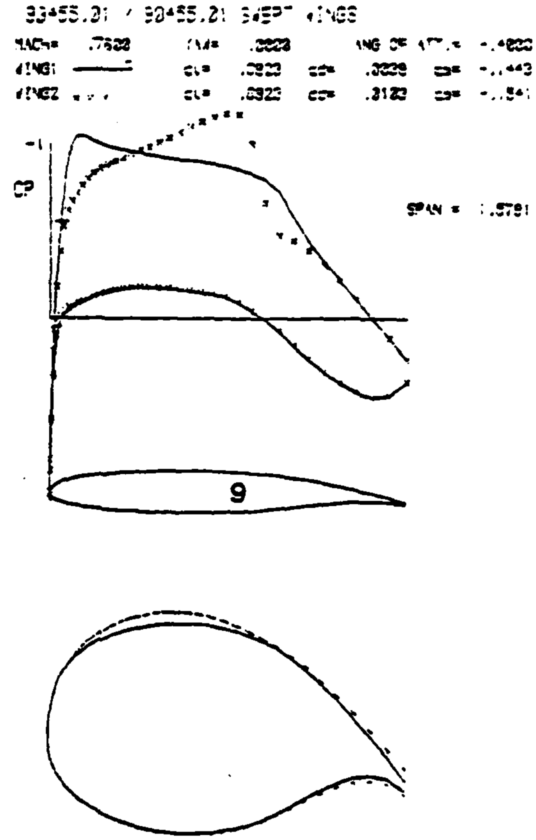

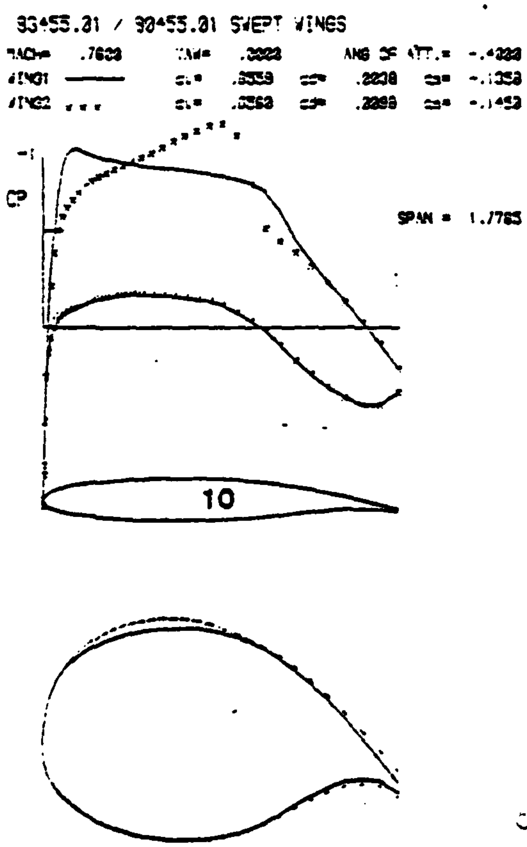

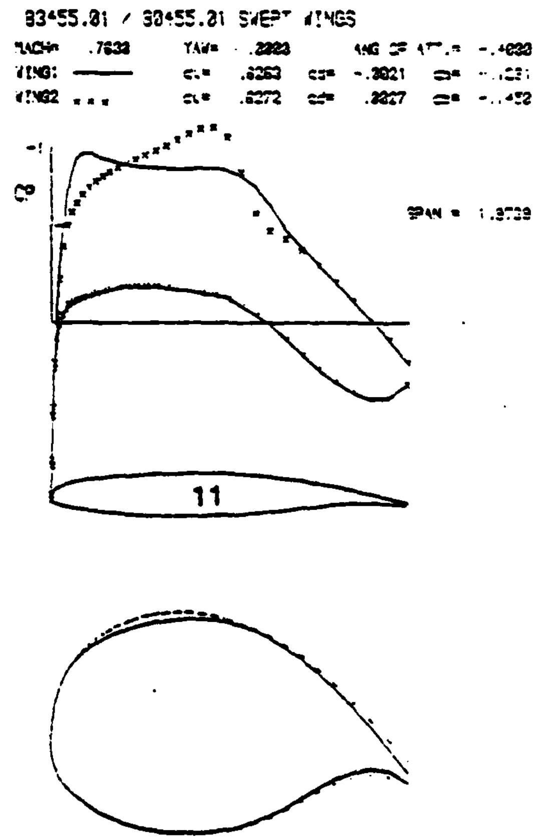

Figure 6 (continued).

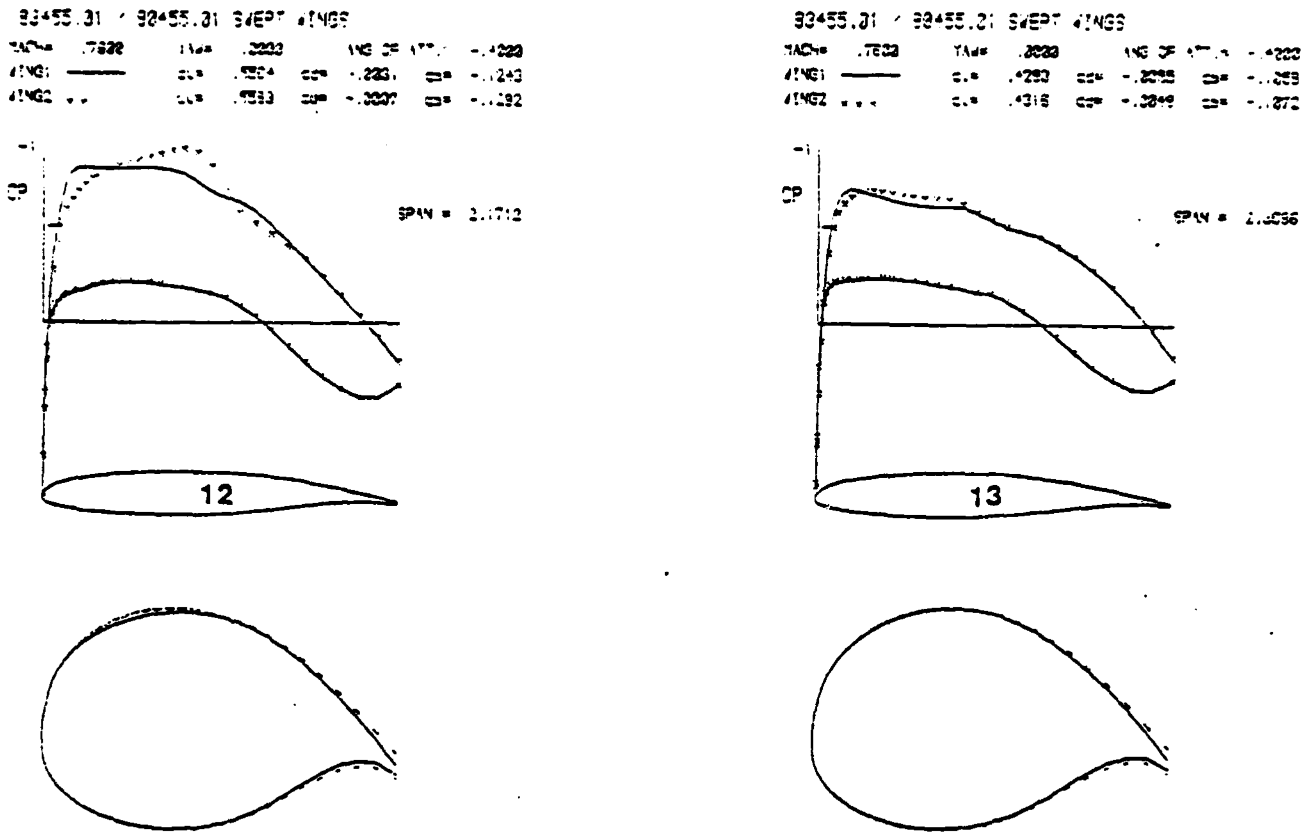

Figure 6 (concluded).